Desalination and Water Treatment
www.deswater.com

doi: 10.1080/19443994.2015.1089420

57 (2016) 18260–18274
August

Taylor & Francis
Taylor & Francis Group

Preparation of polymeric aluminum ferric chloride (PAFC) coagulant from fly ash for the treatment of coal-washing wastewater

Long Yan[a,b,*], Yufei Wang[a,b], Jian Li[a,b], Huidong Shen[a], Chao Zhang[a], Tiantian Qu[a]

[a]*Yulin Engineering Research Center for Industrial Water Treatment, School of Chemistry and Chemical Engineering, Yulin University, 719000 Yulin, China, Tel./Fax: +86 912 3896585; emails: ylyanlong@126.com (L. Yan), wangyufei0003@163.com (Y. Wang), lijian5220@163.com (J. Li), 1076535211@qq.com (H. Shen), 592412517@qq.com (C. Zhang), 1524679747@ qq.com (T. Qu)*

[b]*Shaanxi Key Laboratory of Low Metamorphic Coal Clean Utilization, Yulin University, 719000 Yulin, China*

Received 14 February 2015; Accepted 23 August 2015

ABSTRACT

Fly ash-based polymeric aluminum ferric chloride (PAFC) was prepared from fly ash leached with acid; the PAFC was used as a coagulant to treat coal-washing wastewater. The effects of pH, reaction temperature, and reaction time on coagulant performance were investigated, with optimal conditions determined using response surface methodology. The coagulation mechanism of PAFC was explored by comparing its performance with commercially available polyaluminum chloride (PAC), using scanning electron microscopy and infrared spectroscopy analyses. Results showed that the optimum PAFC preparation conditions were at a pH of 3.60, a reaction temperature of 92˚C, and a reaction time of 2.30 h. Under these conditions, the removal of suspended solids and chemical oxygen demand in treated coal-washing wastewater reached efficiencies of over 81 and 70%, respectively. This means that the prepared PAFC is an effective coal-washing wastewater treatment technique, combining the advantages of polyaluminum and polyferric coagulants.

Keywords: PAFC coagulant; Fly ash; Coal-washing wastewater; COD; SS; Response surface methodology

1. Introduction

Wet coal cleaning requires a lot of water, which retains high concentrations of fine particles after the cleaning process, resulting in increased turbidity and coloring of the wastewater [1,2]. This water is typically referred to as coal-washing wastewater. The surface charge and small particle size (<1 mm) of the particles in the water allow them to avoid significant gravitational sedimentation rates, causing the formation of stable colloidal suspensions [3,4]. In China, a considerable amount of raw coal consists of young and high mud coal; the wastewater generated from this coal has higher concentrations of smaller particles with strongly negative surface charges. This results in a stable colloidal system that is difficult to treat [2]. Developing a chemically non-invasive and low-cost coagulant could surmount these problems and help meet stringent environmental regulations related to the quality of coal-washing wastewater.

A new type of ferro-aluminum composite coagulant, polymeric aluminum ferric chloride (PAFC),

*Corresponding author.

1944-3994/1944-3986 © 2015 Balaban Desalination Publications. All rights reserved.

combines the advantages of polyaluminum and polyferric coagulants while overcoming the disadvantages of polyaluminum chloride (PAC, copious aluminum residue after treatment) and polyferric chloride (PFC, poor stability) [5,6]. Copolymerization of aluminum and iron can increase polymerization and branching of the formed polymers, while adding Al^{3+} and Fe^{3+} ions can also increase the polymer charge. These conditions lead to enhanced adsorption and charge neutralization, considerably improving sweep coagulation effects in wastewater pollutants [7]. Moreover, some research indicates that there is little residual Al and Fe in the aquatic solution after treatment [5,7]. As a result, PAFC has attracted significant attention in the water treatment field, with the significant potential for use in industrial water treatment [8,9].

Fly ash (FA) is a solid waste residue produced from coal combustion in coal-fired power plants; the ash is composed of small, light particles that are kept airborne by the wind when released into the environment [10]. If coal fly ash is directly discharged into the environment, it may cause serious environmental harm by polluting water, the atmosphere, and soil [11]. Some researchers have noted that fly ash is an ideal raw material for the preparation of PAFC, because it is rich in iron oxides and aluminum at an appropriate weight ratio [12,13]. Therefore, fly ash could be converted into a valuable PAFC coagulant for wastewater treatment, reducing operational costs, while improving solid waste disposal [14].

However, despite abundant research into inorganic polymer coagulant preparation, the primary raw materials used in industry are bauxite and calcium aluminate; these are both used for PAC, the most widespread coagulant. Fly ash has not been explored as a raw material at an industrial level, because its composition is very complex and quite variable, making it difficult to control leachate elements [15]. Developing techniques to prepare PAFC using fly ash may result in coagulants that are cost-effective and offer excellent performance. This would also offer a new way to recycle fly ash.

Accordingly, for this study, fly ash-based PAFC coagulants were prepared using the acid leaching of fly ash to facilitate coal-washing wastewater treatment. The effects of pH, reaction temperature, and reaction time on coagulation efficiency were studied. The optimum conditions for preparing PAFC coagulants were also determined using response surface methodology (RSM). The PAFC coagulation mechanism was determined by comparing the coagulation performance of PAFC with commercially available PAC coagulants.

2. Materials and methods

2.1. Materials

Fly ash and coal-washing wastewater samples were obtained from a coal washing plant and a power plant in Yulin, Shaanxi province of China, respectively. This area is one of the world's seven largest coalfields. Table 1 lists the chemical properties of the fly ash, determined using X-ray fluorescence spectroscopy. Table 2 lists the characteristics of the coal-washing wastewater sample. Analytical reagent grade hydrogen peroxide (H_2O_2) and sodium hydroxide (NaOH) were purchased from Chemicals Ltd (Xi'an, China); commercially available polyaluminum chloride (PAC) was purchased from Chemicals Products Co., Ltd (Zhengzhou, China).

2.2. Preparation of PAFC

Previous research [16] was used as the basis for PAFC coagulant preparation, with the addition of 10% H_2O_2 to an acid-leached filtrate of fly ash under optimum conditions (using an orthogonal test). This enabled the complete oxidation of Fe^{2+} to Fe^{3+}, followed by the addition of the remaining materials, as shown in Fig. 1. The stirring speed was maintained and the reaction was heated under reflux. Once the target temperature was attained, sequential drops of 2 M NaOH solution were added to adjust the mixture pH. The mixture was stirred for a set time, naturally cooled to room temperature, aged for 24 h, and then dried at 105℃ to yield the desired powdered PAFC coagulant. To prepare samples for analyses, the PAFC solution was adsorbed onto a copper net, and then dried at room temperature.

2.3. Treatment of coal-washing wastewater using PAFC

PAFC coagulant tests in coal-washing wastewater samples were conducted according to the national standard regulations on wastewater treatment with PAC [17]. The experimental procedure was as follows:

For the mixing step, 500 mL of coal-washing wastewater sample was rapidly stirred at 500 rpm and room temperature in a glass beaker. A defined amount of the prepared powdered PAFC coagulant (0.22 g L^{-1}) was then added while stirring at a constant speed for 5 min. The amount of coagulant was driven by previous research, which showed that this is the level at which the coagulant can dissolve completely in the coal wastewater. For the coagulation step, the mixing speed was adjusted to 60 rpm and

Table 1
Chemical composition of fly ash

Composition	SiO_2	Al_2O_3	Fe_2O_3	CaO	TiO_2	Na_2O	SO_3	Losson ignition
wt%	45.51	21.38	19.36	3.24	0.74	1.32	0.97	1.96

Table 2
Characteristics of coal-washing wastewater sample

Property	Value
Density	1.138 g cm^{-1}
pH	4.72
COD[a]	7,480 mg L^{-1}
Kinematic viscosity	0.045 cm^2 s^{-1}
Color	Aterrimus
Conductivity	944 μS cm^{-1}
SS[b]	12,445 mg L^{-1}
Zeta potential	−0.063 V

[a]COD denotes chemical oxygen demand.
[b]SS denotes suspended solids.

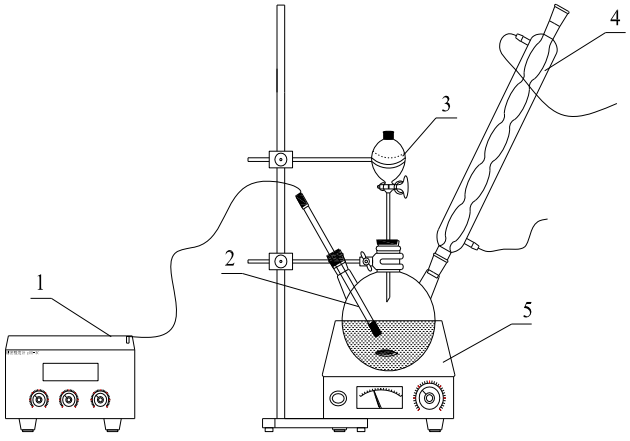

Fig. 1. Experimental setup.
Notes: (1) pH meter, (2) three-neck round-bottom flask, (3) dropping funnel, (4) reflux condenser, and (5) magnetic stirring apparatus.

the mixture was stirred for 30 min to facilitate the reaction.

To facilitate sedimentation, stirring was stopped and the mixture was allowed to stand for 30 min. Then, 10 mL of supernatant was collected to analyze chemical oxygen demand (COD) and the amount of suspended solids (SS) present. Additionally, to study treatment effects, the formation time, shape, size, and sedimentation of the flocs were carefully observed and recorded.

2.4. Analytical methods

A scanning electron microscope (Philips-FEI Model Quanta 200, USA) and FT-IR Spectrophotometer (IRPrestige-21, SHIMADZU, Japan) were used to characterize the structure of the prepared PAFC and the purchased PAC.

The pH of the effluent was monitored with a pH meter (pHS-3C, China), and standard methods were used to measure the COD and SS content of the wastewater before and after the treatment [18,19]. COD was determined using potassium dichromate as the oxidant; the free potassium dichromate was titrated with a standard ferrous ammonium sulfate solution. The SS content was determined as the ratio of the mass of residue on the filter paper to the volume of filtered wastewater. The removal efficiencies R of COD and SS (R_{COD} and R_{SS}) at time t were calculated as follows:

$$R = \frac{c_0 - c_t}{c_0} \times 100\% \quad (1)$$

In this expression, c_0 (mg L^{-1}) is the initial COD or SS value of the non-treated wastewater and c_t (mg L^{-1}) is the COD or SS value measured in the effluent at time t (min).

3. Results and discussion

3.1. Factors influencing PAFC coagulant preparation

Many factors influence PAFC preparation; pH, reaction temperature, and reaction time were selected as the most important factors based on theoretical analyses and several exploratory experiments. Varying the amount of aluminum and iron can also significantly influence PAFC performance. However, we did not consider these parameters, because fly ash was used as the source of aluminum and ferrum.

3.1.1. Effect of pH on PAFC performance

Fig. 2 shows the effect that PAFC (0.22 g L^{-1}) had on a 500-mL coal-washing wastewater sample when the coagulant was prepared at 90°C, the pH was adjusted to different experiment levels using drops of

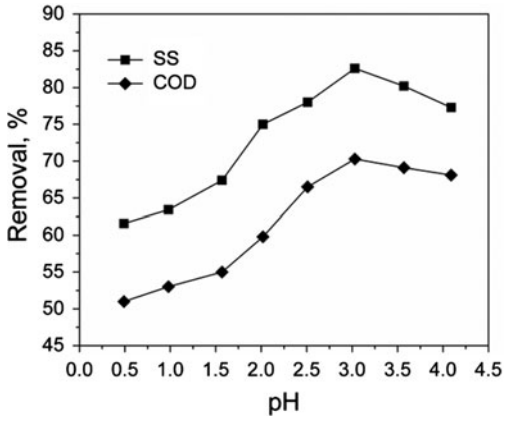

Fig. 2. Effect of pH value on PAFC performance (preparation conditions of PAFC: reaction temperature of 90℃, reaction time of 2 h).

aqueous NaOH, the mixture was stirred at a constant temperature for 2 h, and then the mixture was allowed to stabilize under static conditions. Increasing the pH initially improved the COD and SS removal efficiencies; as the pH continued to increase, removal efficiencies decreased again. The optimum pH was 3. The prepared PAFC has Al^{3+} and Fe^{3+} intermediates after hydrolysis, polymerization, and precipitation. These steps can be influenced by the pH value and the concentration of Al^{3+} and Fe^{3+} [5,20,21].

This indicates that after the addition of NaOH, the Al^{3+} and Fe^{3+} in the acid-leached fly ash solution are hydrolyzed with coordinated water. The metals then undergo polycondensation to form a polynuclear coordinated polymer; as such, the basicity of the PAFC coagulants changes during preparation [20]. Basicity represents the number of hydroxyl groups polymerized with Al^{3+} and Fe^{3+} in the molecular structure; these groups directly influence properties such as the degree of polymerization, amount of charge, and the effect and stability of the coagulation. The basicity B of the PAFC coagulant is defined as $B = [OH]/[Al_T + Fe_T]$, where [OH] is the amount of hydroxyl groups, driven by the amount of NaOH added to the solution during PAFC preparation. The parameter $[Al_T + Fe_T]$ represents the total equivalent concentration of aluminum and ferrum in the acid-leached solution [5–7].

Based on this equation, the basicity of the PAFC coagulant and abundance of hydroxyl groups increases with increasing pH. This indicates that a higher pH value should increase the treatment performance. However, when the pH exceeded 3, the coagulation effect decreased, consistent with other studies [8,22–24]. This may be due to the higher polymerization rate of the leached Fe^{3+} ions, compared with Al^{3+}. This higher rate results in the migration of Fe^{3+} from high polymeric hydroxy complex ions with high valence to high polymeric coagulation products with low valence [25]. Hence, in subsequent experiments, the pH was maintained at 3.

3.1.2. Effect of reaction temperature on PAFC performance

Fig. 3 shows the effect of the reaction temperature on PAFC (0.22 g L^{-1}) performance when applied to a 500-mL coal-washing wastewater sample at a pH of 3.

As Fig. 3 shows, the COD and SS removal efficiencies were improved by increasing reaction temperatures during PAFC preparation. The polymerization of Al^{3+} and Fe^{3+} during PAFC preparation are endothermic processes. Thus, higher temperatures benefit the polymerization reaction, and accelerate the generation of the mono polymer, leading to improved coagulation effects [5,6,26]. However, temperatures above 90℃ result in an increased chain transfer rate, k_t, that is higher than the chain growth rate, k_p. This contributes to a relatively stable coagulation from the product [27]. Furthermore, maintaining high operating temperatures is inconvenient and can incur higher costs. Thus, 90℃ was selected as the optimal reaction temperature.

3.1.3. Effect of reaction time on PAFC performance

Fig. 4 shows the effect of reaction time on coagulation performance. A 500-mL coal-washing wastewater sample, and a PAFC concentration of 0.22 g L^{-1} were

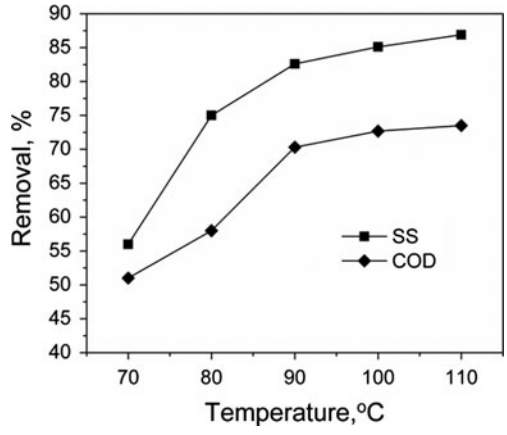

Fig. 3. Effect of reaction temperature on PAFC performance (preparation conditions of PAFC: pH of 3, reaction time of 2 h).

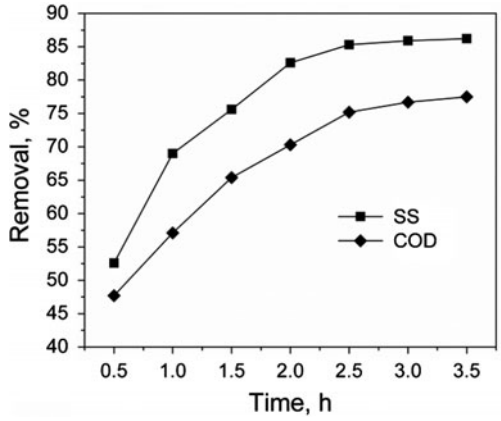

Fig. 4. Effect of reaction time on PAFC performance (preparation conditions of PAFC: reaction temperature of 90℃, pH of 3, reaction time of 2 h).

used; the reaction temperature was 90℃, and the pH was held at 3.

Reaction time is an important parameter in the reaction process, as it influences coagulation ability and production capacity. As Fig. 4 shows, the COD and SS removal efficiencies, which indicate PAFC coagulation performance, were relatively low when the reaction time was too short. When the reaction time is too short, heat absorption is insufficient; as such, polymerization of the prepared PAFC is limited. Extending the reaction time allows sufficient time for polymerization, improving the coagulation effect of the PAFC in the coal-washing wastewater. Stable COD and SS removal efficiencies after 2.5 h indicated the completion of the polymerization process. After this time point, extending the reaction time further would waste power resources without improving production efficiency. Therefore, selecting the best reaction time is key to achieving optimal polymerization and maintaining reasonable energy consumption and production costs.

In summary, the pH, reaction temperature, and reaction time used to prepare PAFC coagulants influenced the resulting coagulation effect in coal-washing wastewater samples to different degrees. However, these "single-factor experiments," where only one factor is adjusted while the others are kept constant, are not sufficient to effectively determine optimum conditions for PAFC coagulant preparation.

3.2. Optimizing PAFC preparation conditions using RSM

RSM is a modeling method used to determine the contribution and interaction of factors on the target response value to support optimization [28–31]. Based on the experimental results above, Design Expert software and RSM Box–Behnken Design were used to further study the effects of pH, reaction temperature, and reaction time on the COD and SS removal efficiencies. PAFC preparation conditions were as follows: the pH ranged from 2 to 4, reaction temperatures ranged from 70 to 110℃, and reaction time ranged from 0.5 to 3.5 h. Table 3 shows the factors and their levels. The coagulants prepared under these different conditions were aged for 24 h and dried at 105℃. A 500-mL coal-washing wastewater sample and PAFC amount of 0.22 g L^{-1} were used.

3.2.1. Response surface models and regression significance tests

Table 3 shows the RSM design, which was a three-level experiment with three variables. Table 4 shows the experimental design and analysis results. Predicted values were estimated by the software using regression analysis, based on the experimental data. The relative error was calculated as the ratio of absolute error to the actual value; the absolute error was calculated as the difference between the actual value and the predicted value. Table 4 shows that the difference between the predicted value and actual value was always less than 5%. Fig. 5 compares the actual and predicted values; the actual value distribution was fitted to the predicted value distribution. These results illustrate that the model is appropriate for determining the optimum conditions for preparing PAFC.

Second-degree polynomial regression fitting was applied to the experimental data in Table 4, using ANOVA in Design Expert. The RSM regression coefficients and variance analyses are shown in Tables 5 and 6, respectively. F and p are defined in the table footnotes. The p-values of less than 0.05 for the associated model item or regression indicate a statistically significant model result; a "lack of fit" reflected a discrepancy between the actual value and the modeled value. The model can only be used to simulate the experiment if the "lack of fit" value is more than 0.1

Table 3
Coding of test factors and levels

	Level		
Factor	−1	0	1
A (pH)	2	3	4
B (Temperature, ℃)	70	90	110
C (Time, h)	0.5	2	3.5

Table 4
Response surface design and test results

No.	Factors			SS removal efficiency (%)			COD removal efficiency (%)		
	A	*B*	*C*	Actual value	Predicted value	Relative error (%)	Actual value	Predicted value	Relative error (%)
1	−1	−1	0	59.47	58.93	0.91	49.51	48.62	1.80
2	1	−1	0	65.8	65.50	0.46	54.1	53.91	0.35
3	−1	1	0	64.8	65.10	−0.47	58.7	58.89	−0.32
4	1	1	0	70.8	71.34	−0.77	60.8	61.69	−1.47
5	−1	0	−1	51.7	50.97	1.40	46.2	46.10	0.21
6	1	0	−1	62.9	61.93	1.54	55	54.20	1.45
7	−1	0	1	69.15	70.12	−1.40	61.5	62.30	−1.30
8	1	0	1	71.24	71.97	−1.02	62.2	62.30	−0.15
9	0	−1	−1	40.23	41.50	−3.16	30.75	31.74	−3.22
10	0	1	−1	47.82	48.24	−0.88	44.1	44.01	0.21
11	0	−1	1	57.24	56.82	0.74	47.03	47.12	−0.20
12	0	1	1	63.37	62.10	2.00	53.9	52.91	1.83
13	0	0	0	82.5	81.70	0.96	70.3	70.42	−0.17
14	0	0	0	81.98	81.70	0.34	69.45	70.42	−1.39
15	0	0	0	81.33	81.70	−0.46	71.5	70.42	1.52
16	0	0	0	82.15	81.70	0.54	70.13	70.42	−0.41
17	0	0	0	80.56	81.70	−1.42	70.7	70.42	0.40

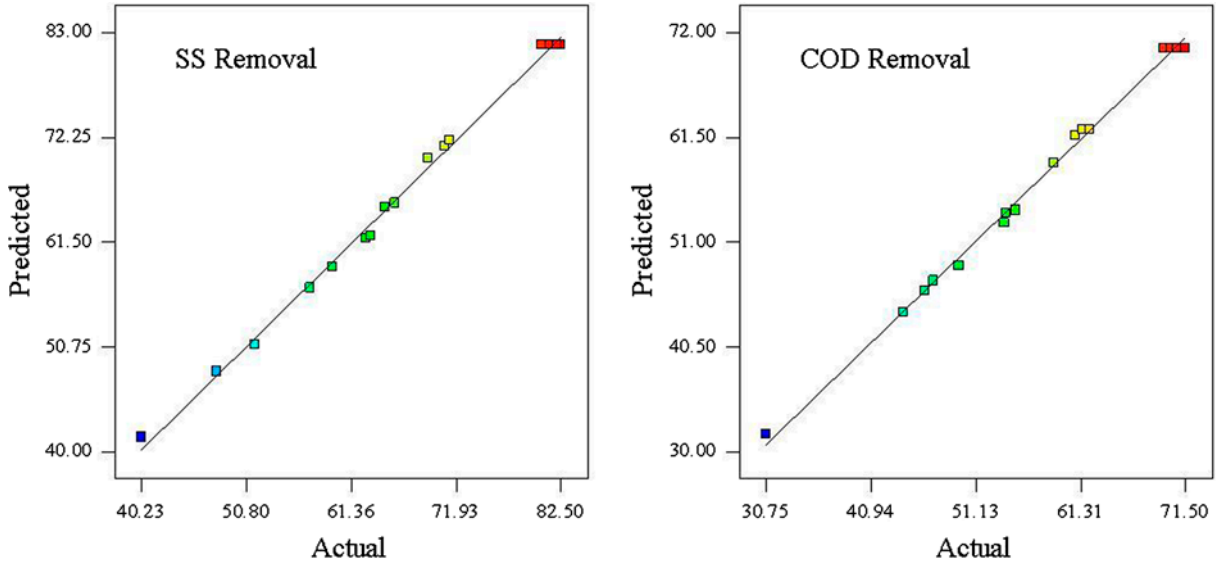

Fig. 5. Relationship between the actual and predicted.

[32]. *F*-values indicating a "lack of fit" describe data variation around the fitted model. If the model does not fit the data well, this is significant [33].

The SS and COD removal efficiency regression models generated *p*-values of 0.1026 and 0.1667 (Table 4), respectively; the *F*-statistic was statistically insignificant but the "lack of fit" was not obvious, implying a correlation between the variables and process responses. Additionally, following simulated regression equations for SS and COD removal efficiencies, we found that *A*, *B*, *C*, *AC*, A^2, B^2, and C^2 in the regression equation for SS removal efficiency and *A*, *B*, *C*, *AC*, *BC*, A^2, B^2, and C^2 in the regression equation for COD were significantly influenced. The second-degree polynomial regression equations for SS and COD removal efficiencies are as follows:

Table 5
Regression Coefficients and Significance Test of SS Removal Efficiency

Item	Coefficient estimates	Standard deviation	Average sum	Mean square	F^a	p^b	Significance[c]
Model			2,615.53	290.61	211.07	<0.0001	*S*
Lack of fit			7.28	2.43	4.12	0.1026	*N*
Intercept	81.70	0.52					
A	3.20	0.41	82.05	82.05	59.59	0.0001	*S*
B	3.00	0.41	72.30	72.30	52.51	0.0002	*N*
C	7.29	0.41	425.59	425.59	309.10	<0.0001	*S*
AB	−0.08	0.59	0.03	0.027	0.020	0.8921	*N*
AC	−2.28	0.59	20.75	20.75	15.07	0.0060	*S*
BC	−0.37	0.59	0.53	0.53	0.39	0.5536	*N*
A^2	−2.45	0.57	25.31	25.31	18.39	0.0036	*S*
B^2	−14.03	0.57	829.34	829.34	602.33	<0.0001	*S*
C^2	−15.50	0.57	1,012.17	1,012.17	735.12	<0.0001	*S*
R^2	0.9963						

[a]*F* denotes the ratio of the mean square deviation of regression to the mean square of error.
[b]*p* denotes the associated probability of *F*.
[c]*S* denotes that the effect of an item is significant; *N* denotes that the effect of an item is non-significant.

Table 6
Regression coefficients and significance test of COD removal efficiency

Item	Coefficient estimates	Standard deviation	Average sum	Mean square	F^a	p^b	Significance[c]
Model			2,106.49	234.05	227.02	<0.0001	*S*
Lack of fit			4.93	1.64	2.88	0.1667	*N*
Intercept	70.42	0.45					
A	2.02	0.36	32.76	32.76	31.78	0.0008	*S*
B	4.51	0.36	162.99	162.99	158.10	<0.0001	*S*
C	6.07	0.36	295.00	295.00	286.14	<0.0001	*S*
AB	−0.62	0.51	1.55	1.55	1.50	0.2598	*N*
AC	−2.03	0.51	16.40	16.40	15.91	0.0053	*S*
BC	−1.62	0.51	10.50	10.50	10.18	0.0153	*S*
A^2	−1.18	0.49	5.86	5.86	5.68	0.0487	*S*
B^2	−13.46	0.49	762.74	762.74	739.83	<0.0001	*S*
C^2	−13.01	0.49	712.87	712.87	691.45	<0.0001	*S*
R^2	0.9966						

[a]*F* denotes the ratio of the mean square deviation of regression to the mean square of error.
[b]*p* denotes the associated probability of *F*.
[c]*S* denotes that the effect of an item is significant; *N* denotes that the effect of an item is non-significant.

$$\text{SS}\ (\%) = 81.70 + 3.20A + 3.01B + 7.29C - 0.083AB - 2.28AC - 0.37BC - 2.45A^2 - 14.03B^2 - 15.50C^2 \quad (2)$$

$$\text{COD}\ (\%) = 70.42 + 2.02A + 4.51B + 6.07C - 0.62AB - 2.02AC - 1.62BC - 1.18A^2 - 13.46B^2 - 13.01C^2 \quad (3)$$

The correlation index R^2, represents the degree of fit of the regression equation [34,35], with values of 0.9963 and 0.9966 for SS and COD removal efficiencies, respectively. This means that 99.63% of the SS removal efficiency variation and 99.66% of the COD removal efficiency variation can be explained by the model. The model was statistically significant, with a high degree of fit. Therefore, based on SS and COD removal efficiencies, the optimized conditions for PAFC coagulant preparation can be predicted within a suitable range [36].

3.2.2. Response surface analysis

To determine optimum conditions for PAFC coagulant preparation, three-dimensional response surface and contour plots were drawn, based on the influence of the two factors from the model equations of the SS and COD removal efficiencies (as shown in Figs. 6–8). The plots were used to determine the factors and their combined effects on SS and COD removal efficiencies.

The response surface graph in Fig. 6 shows that the pH and reaction temperature significantly influenced SS and COD removal efficiencies; there was an initial increase, followed by a decrease. When the pH exceeded 3.5, the SS and COD removal efficiencies did not change considerably. However, removal efficiencies sharply declined when the reaction temperature rose above 95℃. Therefore, we can conclude that the effect of the reaction temperature and the combined effect of temperature and pH are statistically significant. The contour analysis in Fig. 6 indicates the corresponding optimal conditions. The oval zone indicates that the optimal pH range is 2.5–4 and the optimal reaction temperature is 85–105℃; these levels correspond to SS and COD removal efficiencies of 78.91

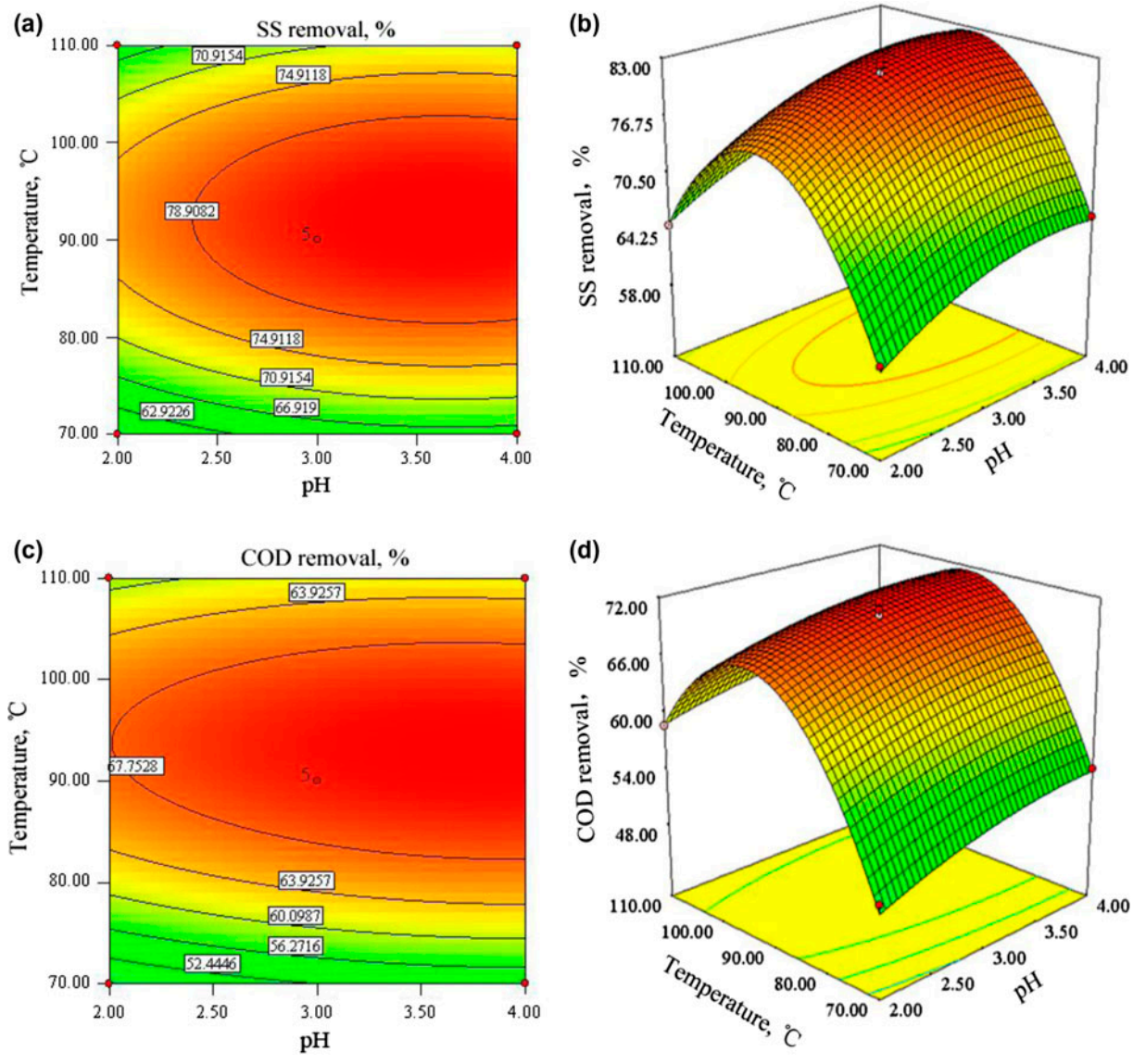

Fig. 6. DESIGN-EXPERT plot of SS and COD removal showing the effect of pH and reaction temperature. (a and c) Contour and (b and d) response surface plots.

and 67.75%, respectively. Additionally, variations in the COD and SS removal efficiencies were similar. This indicates that the COD of the coal-washing wastewater sample was linked to the superfine SS.

Fig. 7 shows the interactive effects of pH and reaction time on the SS and COD removal efficiencies. The response surface graph shows that pH influenced the SS and COD removal efficiencies less than reaction time. However, SS and COD removal efficiencies continued to increase with an increase in the pH. The effect of reaction time was also significant. The SS and COD removal efficiencies first increased, then decreased once the reaction time exceeded 2.75 h. The combined effects of pH and reaction time on SS and COD removal efficiencies were also significant. Analyzing contour lines showed that the optimal COD removal efficiency occurred within a pH range of 2.5–4.0; the optimum SS removal efficiency occurred within a pH range of 2.0–4.0. The optimum reaction time was 1.5–3.0 h for both factors.

Based on results to this point, it was determined that the effects of the "single-factor experiments" were, and SS and COD could be removed simultaneously. Therefore, the crimson oval zone (with a pH range of 2.5–4.0 and a reaction time of 1.5–3.0 h) was identified as the optimal area. Within this area, the SS and COD removal efficiencies reached 77.92 and 67.41%, respectively.

Fig. 8 presents the interactive effects of reaction temperature and time on SS and COD removal efficiency. Both reaction temperature and time significantly influenced removal efficiency; as reaction temperature and reaction time increased, SS and COD removal efficiencies first increased, and then decreased. The most distinct decrease in efficiency occurred when the temperature ranged 95–100℃ and the reaction time was 2.75 h. A contour line analysis was used to identify an optimal region for SS and COD removal efficiency. The resulting red zone is bounded by a reaction temperature range of 80–105℃ and reaction time range of 1.25–3.25 h. Within this area, the SS and COD removal efficiencies were 75.84 and 64.82%, respectively.

A lighter red hue was observed when compared with the results in Figs. 6 and 7, and the area is spherical rather than elliptical. This indicates that the combined effects generated within this region were weaker than those displayed in Figs. 6 and 7. The shape of the contour line reflects the intensity of the combined effect; an ellipse indicates a relatively strong combined effect, whereas a circle suggests a relatively weak one [37].

3.2.3. Verification

Design Expert software was used for the model optimization analysis to determine the best PAFC preparation conditions to generate the highest SS and COD removal efficiencies. The optimum conditions were when the pH was 3.60; the reaction temperature was 92.47℃; and the reaction time was 2.28 h. The corresponding SS and COD removal efficiencies were 83.45 and 71.93%, respectively. These data were obtained from the first derivation of the regression equations (Eqs. (2) and (3)).

Model validity was assessed experimentally. A 500-mL coal-washing wastewater sample was treated with PAFC coagulants (0.22 g L^{-1}) prepared at a pH of 3.60, at a temperature of 92℃, and with a reaction time of 2.30 h. Table 7 shows experimental results; the experiment was conducted in triplicate. As observed, SS and COD removal efficiencies exceeded 81 and 70%, respectively; the difference between relative error and predicted value was no more than 3% [32]. This indicates that the model can be effectively used to predict the success of different preparations of PAFC coagulants.

3.3. Mechanistic comparison between PAFC and PAC

PAC is currently the most widely inorganic polymer coagulant [38]. However, problems exist with this composite, including the need for large dosages, minimal effects, small and dense coagulants, slow sedimentation rates, and residual aluminum in water. As a composite coagulant, PAFC combines PAC and the aggregated state of iron, merging the advantages of aluminum and iron coagulants. PAFC can increase molecular structures, and improve electrical neutralization, adsorption bridging, and sedimentation functions in the wastewater treatment process. Accordingly, it is important to compare the properties and structures of PAC and PAFC.

3.3.1. Coagulation effect

To study the PAFC coagulating mechanism, different doses of experimentally prepared PAFC and commercially available PAC were used to treat separate 500-mL coal-washing wastewater samples (Fig. 9).

As Fig. 9 shows, PAFC and PAC significantly determined the coagulation effect. As coagulant dosages increased, the SS and COD removal efficiencies increased rapidly, then decreased sharply after attaining maximum efficiency. Adding PAFC and PAC neutralizes the surface charge of the coal-washing

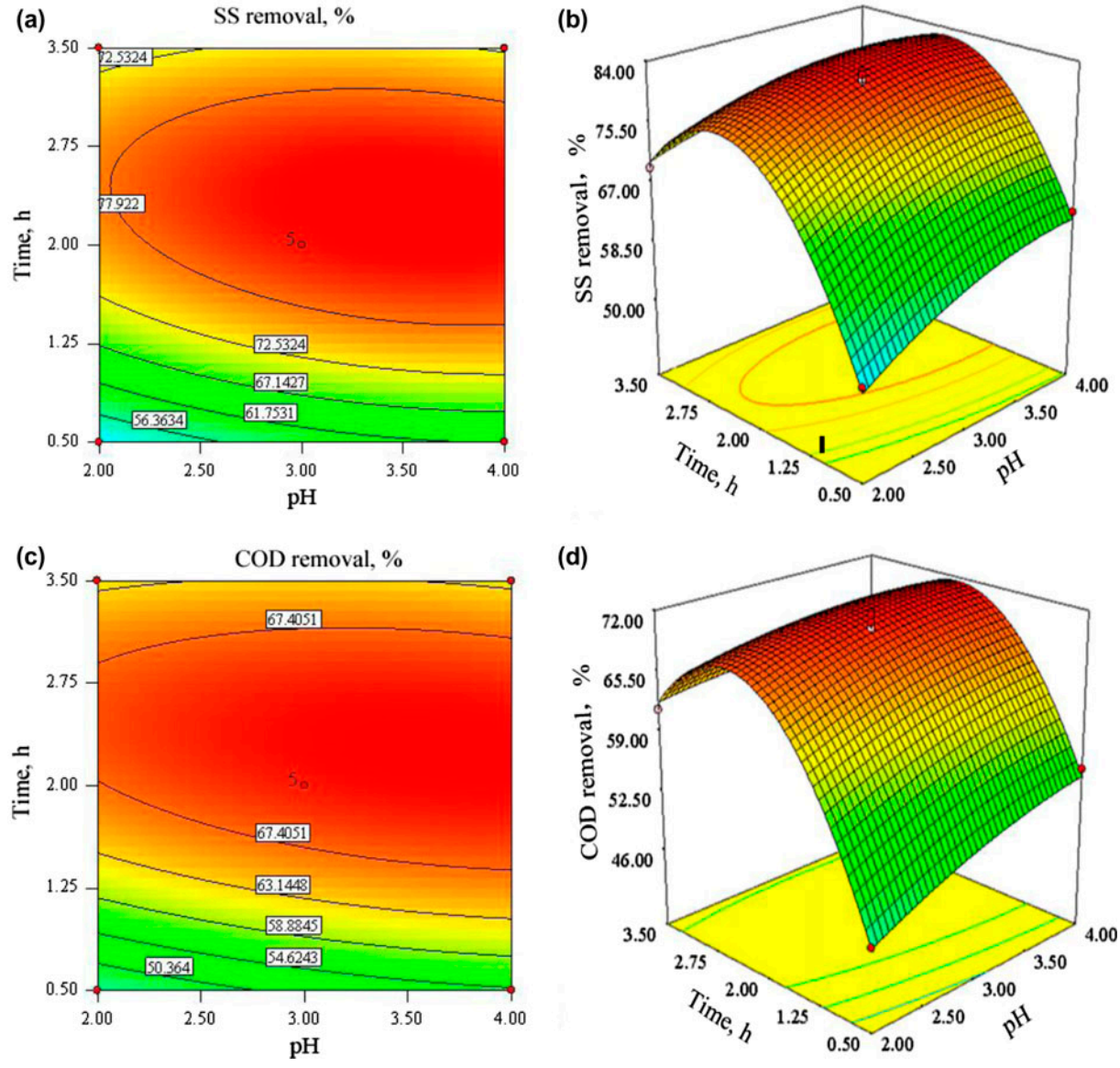

Fig. 7. DESIGN-EXPERT plot of SS and COD removal showing the effect of pH and reaction time. (a and c) Contour and (b and d) response surface plots.

wastewater colloids, disrupting the colloidal stability needed to generate flocculating constituents.

If the coagulant dose is too low, the colloid surface charge cannot be neutralized, resulting in reduced SS and COD removal efficiencies. In contrast, excessively high coagulant dosages waste resources and generate negative charges on the colloid surface. Hence, establishing an optimal coagulant dosage is vital to maximize coagulation effects in coal-washing wastewater treatment processes.

Using PAFC coagulants yielded higher SS and COD removal efficiencies than using PAC coagulants. Additionally, flocculation time, the sizes of the formed flocs, and sedimentation rate were better with PAFC than with PAC. Because PAFC combines the advantages of PAC and polyferric sulfate inorganic polymer coagulants, it has broader application prospects and achieves higher performance.

3.3.2. Scanning electron microscopy (SEM) analysis

The morphology and structure of the PAC and PAFC coagulants were observed using scanning electron microscopy (SEM); Fig. 10 displays the results.

The commercially available PAC particles are relatively large and loosely assembled; whereas PAFC

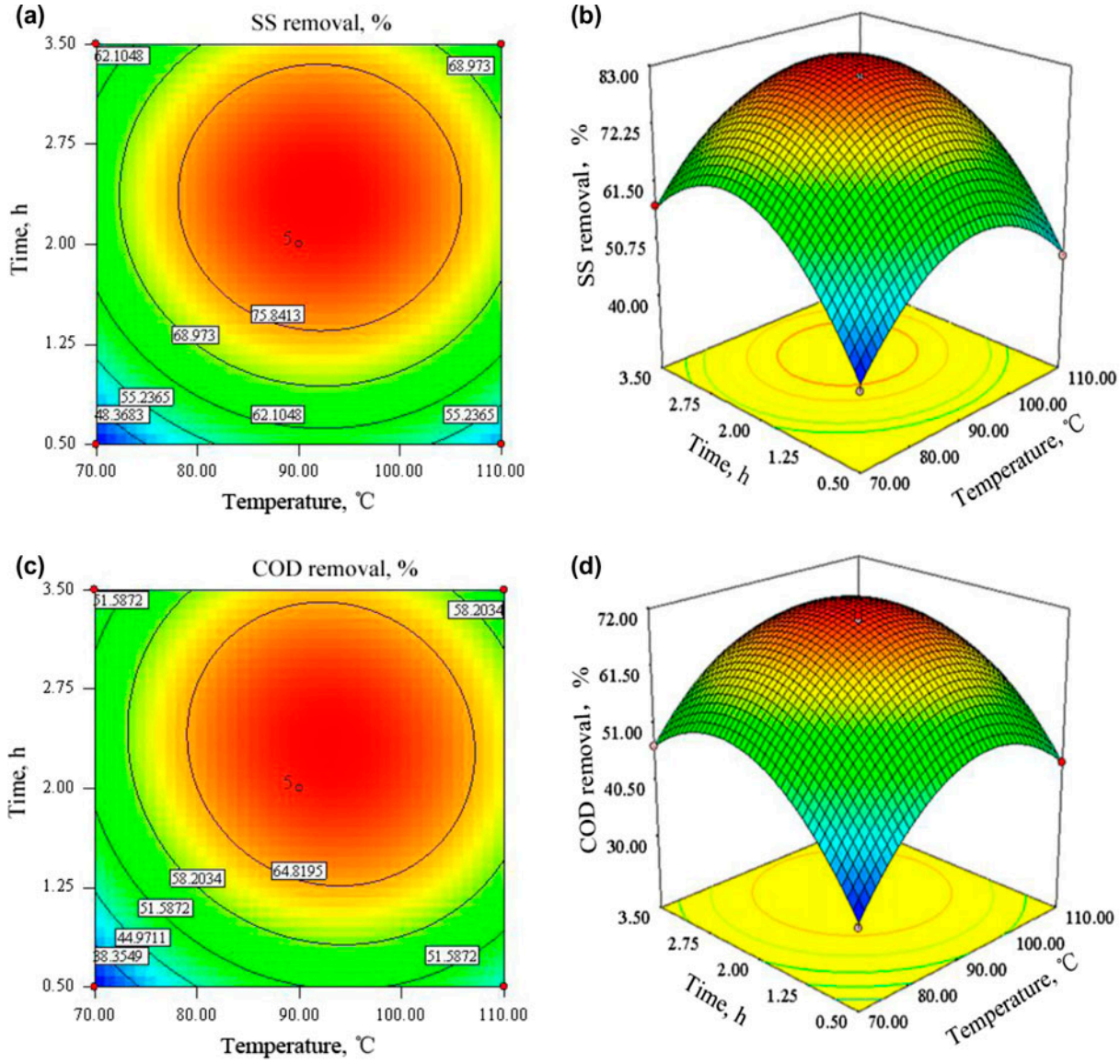

Fig. 8. DESIGN-EXPERT plot of SS and COD removal showing the effect of reaction temperature and reaction time. (a and c) contour and (b and d) response surface plots.

Table 7
Comparison of the SS and COD removal efficiencies obtained from the model and determined experimentally

	SS removal efficiency (%)			COD removal efficiency (%)		
Experiment no.	Predicted value	Actual value	Relative error (%)	Predicted value	Actual value	Relative error (%)
1	83.45	81.86	1.91	71.93	70.64	1.80
2		81.40	2.46		70.24	2.35
3		81.14	2.77		70.15	2.47

particles are smaller and closely assembled with numerous crevices. This indicates that PAFC has a larger density than PAC. When compared with commercially available PAC, the prepared PAFC had a larger specific surface area. This likely improved the level of contact with coal slurry particles when

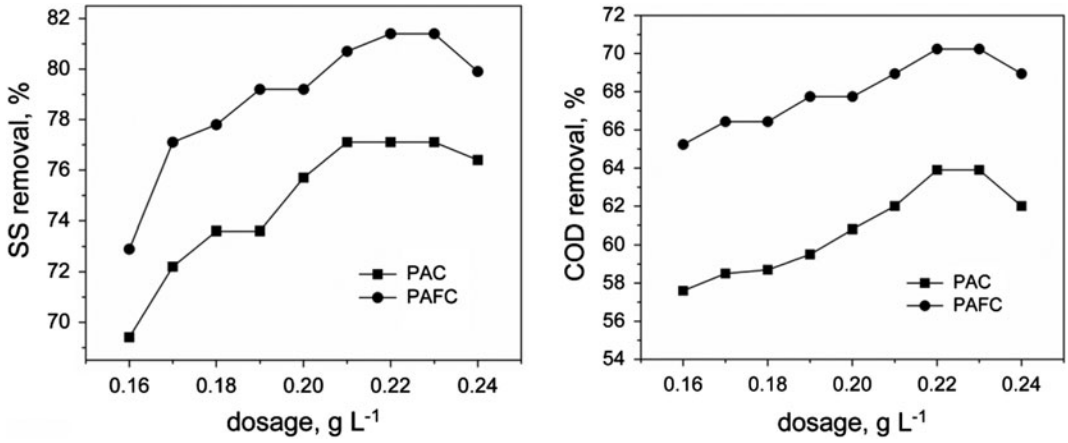

Fig. 9. SS and COD removal efficiencies as a function of PAC and PAFC dosage (flocculation conditions: pH_i of 4.72, room temperature of 25 ± 2°C, flocculation time of 30 min).

treating the coal-washing wastewater sample. Both PAFC and PAC have a net structure that can assemble smaller particles in the wastewater treatment process, according to the coagulation mechanism. Hence, the formed coagulant from PAFC was large enough to adsorb and trap the pollutants. As such, a high sedimentation rate was obtained and the treatment effect was relatively good.

3.3.3. FT-IR spectra analysis

To confirm the presence of polyaluminum and polyferric sulfate in PAFC and to assess the differences between PAFC and commercially available PAC, samples were dried at 105°C and ground prior to FT-IR analysis. Potassium bromide was used as the parent material. Fig. 11 shows the FT-IR spectra of the PAC and PAFC coagulants.

Comparing the spectra in Fig. 11 revealed that the commercially available PAC and the prepared PAFC featured similar structures. PAC displayed a broad band at 3,400 cm^{-1}, attributed to adsorbed water molecules. An absorption peak at 1,650 cm^{-1} indicates the presence of coordinated water molecules and OH groups that were connected to the aluminum ion. PAFC spectra also displayed the above-mentioned peaks at the corresponding wave numbers; the peak areas were relatively large, indicating numerous

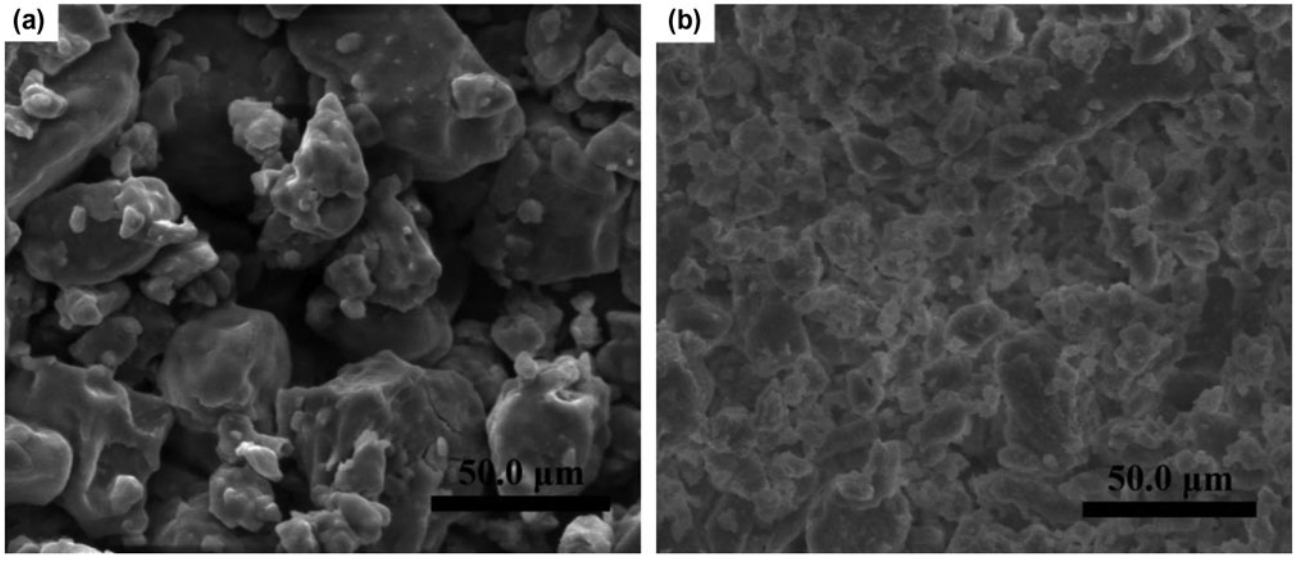

Fig. 10. SEM images of (a) PAC and (b) PAFC flocculant.

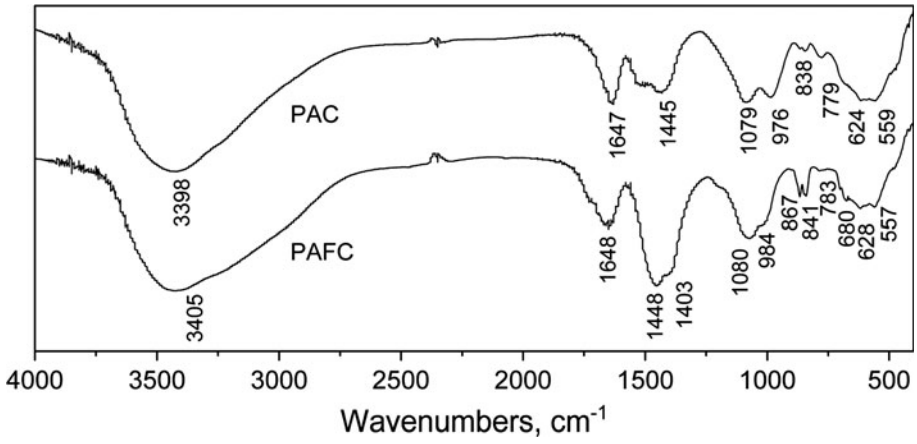

Fig. 11. IR spectrum of PAC and PAFC flocculant.

hydroxyl groups and coordinated water in the prepared PAFC. The adsorption peak at 1,080 cm^{-1} was used as the reference peak to evaluate the extent of coagulant polymerization. The PAC sample displayed a stretching vibration in the Al–OH–Al plane of the polymer; the prepared PAFC displayed stretching vibrations in both the Al–OH–Al and Fe–OH–Fe planes of the polymer. This suggests that the prepared PAFC is structurally similar to the commercially available PAC; a hydrolytic copolymer is formed upon bonding with the hydroxyl with a relatively high degree of polymerization [7].

Further comparing these two types of coagulants revealed that only the bending vibrating peak in the Al–OH–Al plane occurred at 980 cm^{-1} for PAC. In contrast, PAFC displayed bending vibrating peaks in both the Al–OH–Al plane at 980 cm^{-1} and the Fe–OH–Fe plane at 867 cm^{-1}. Moreover, PAC only displayed the integral bending vibrating peak of Al–OH–Al at 624 cm^{-1}, whereas PAFC also displayed the integral bending vibrating peak of Fe–OH–Fe. This illustrates that both, the polymer with the hydroxyl group connected to the aluminum, and the polymer with the hydroxyl group connected to iron, exist in PAFC. Furthermore, a new type of polymer was formed, which differs from the polymer resulting from simply mixing the aluminum and ferrum salts [7]. The excellent polymerization between aluminum and ferrum from fly ash enabled highly efficient PAFC coagulants for treating coal-washing wastewater.

4. Conclusion

PAFC coagulants were prepared from acid-leached fly ash filtrate, and used to treat coal-washing wastewater. Experiments studied the effects of pH, reaction temperature, and reaction time on PAFC coagulation efficiencies. Optimum conditions for the preparation of PAFC coagulants were also determined using RSM. Comparing the morphology, chemical structure, and coagulation performance of the prepared PAFC and commercially available PAC coagulants showed that the prepared PAFC coagulants matched the combined performances of both the PAC and polyferric sulfate components. Therefore, using fly ash-based PAFC is at least as feasible as using conventional coagulants in coal-washing wastewater treatment plants. Using PAFC may reduce the consumption of primary raw materials, including bauxite and calcium aluminate, and support the environment by solving solid waste disposal problems.

Acknowledgments

This work was sponsored in part by National Natural Science Foundation of China (21203163), Science and Technology Plan Project of Shaanxi Province of China (2014KJXX-78, 2014KW16), Science and Technology Plan Project of Yulin Government (Sf13-09, Gy1309), and Scientific Research Project of Yulin University (12GK03, 11GK36).

References

[1] S. Mohanta, B.K. Mishra, S.K. Biswal, An emphasis on optimum fuel production for Indian coal preparation plants treating multiple coal sources, Fuel 89 (2010) 775–781.
[2] Z. Huang, Y. Li, D. Lu, Z. Zhou, Z. Wang, J. Zhou, K. Cen, Improvement of the coal ash slagging tendency by coal washing and additive blending with mullite generation, Energy Fuels 27 (2013) 2049–2056.

[3] T.J. Johnson, E.J. Davis, Electrokinetic clarification of colloidal suspensions, Environ. Sci. Technol. 33 (1999) 1250–1255.
[4] R.A. Garcia, S.A. Riner, G.J. Piazza, Design of a laboratory method for rapid evaluation of experimental flocculants, Ind. Eng. Chem. Res. 53 (2014) 880–886.
[5] Y.Y. Hu, C.Q. Tu, H.H. Wu, Species distribution of polymeric aluminium-ferrum—Timed complexation colorimetric analysis method of Al–Fe-Ferron, J. Environ. Sci. 13 (2001) 418–420.
[6] J.Q. Jiang, N.J.D. Graham, Development of optimal poly-alumino-iron sulphate coagulant, J. Environ. Eng. 129 (2003) 699–708.
[7] G. Zhu, H. Zheng, Z. Zhang, T. Tshukudu, P. Zhang, X. Xiang, Characterization and coagulation–flocculation behavior of polymeric aluminum ferric sulfate (PAFS), Chem. Eng. J. 178 (2011) 50–59.
[8] K.E. Lee, N. Morad, T.T. Teng, B.T. Poh, Development, characterization and the application of hybrid materials in coagulation/flocculation of wastewater: A review, Chem. Eng. J. 203 (2012) 370–386.
[9] A. Matilainen, M. Vepsäläinen, M. Sillanpää, Natural organic matter removal by coagulation during drinking water treatment: A review, Adv. Colloid Interface Sci. 159 (2010) 189–197.
[10] H. Liu, Z. Liu, Recycling utilization patterns of coal mining waste in China, Resour. Conserv. Recycl. 54 (2010) 1331–1340.
[11] Z. Zhao, Q. Du, G. Zhao, J. Gao, H. Dong, Y. Cao, Q. Han, P. Yuan, L. Su, Fine particle emission from an industrial coal-fired circulating fluidized-bed boiler equipped with a fabric filter in China, Energy Fuels 28 (2014) 4769–4780.
[12] A. Seidel, Y. Zimmels, Mechanism and kinetics of aluminum and iron leaching from coal fly ash by sulfuric acid, Chem. Eng. Sci. 53 (1998) 3835–3852.
[13] M. Fan, R.C. Brown, J. Van Leeuwen, M. Nomura, Y. Zhuang, The kinetics of producing sulfate-based complex coagulant from fly ash, Chem. Eng. Process. 42 (2003) 1019–1025.
[14] S. Wang, Y. Boyjoo, A. Choueib, Z.H. Zhu, Removal of dyes from aqueous solution using fly ash and red mud, Water Res. 39 (2005) 129–138.
[15] M. Ahmaruzzaman, A review on the utilization of fly ash, Prog. Energy Combust. Sci. 36 (2010) 327–363.
[16] L. Yan, Y. Wang, H. Ma, Z. Han, Q. Zhang, Y. Chen, Feasibility of fly ash-based composite coagulant for coal washing wastewater treatment, J. Hazard. Mater. 203–204 (2012) 221–228.
[17] General Administration of Quality Supervision, Inspection and Quarantine (AQSIQ), Water Treatment Chemical-Poly aluminium chlorid (GB 15892-2003), Beijing, 2003.
[18] State Environmental Protection Agency (SEPA), Water Quality-Determination of the Chemical Oxygen Demand-Dichromate Method (GB 11914-89), Beijing, 1989.
[19] State Environmental Protection Agency (SEPA), Water Quality-Determination of Suspended Substance-Gravimetric Method (GB 11901-89), Beijing, 1989.
[20] J. Kenneth (Ed.), The Scientific Basis of Flocculation, Sijthoff & Noordboff, Netherlands, 1978.
[21] X. Zhang, Y. Zhao, H. Fan, G. Yang, Y. Lu, Da. Huang, Study of polyaluminium ferric chloride (PAFC) aqueous solutions visible spectra: The RELATIONSHIP among their absorbance at 460 nm, basicities and total Fe concentration of PAFC solutions, Spectrosc. Spect. Anal. 20 (2000) 577–580.
[22] P.M. Bertsch, Conditions for Al13 polymer formation in partially neutralized aluminum solutions1, Soil Sci. Soc. Am. J. 51 (1987) 825–833.
[23] T. Iwahiro, Y. Nakamura, R. Komatsu, Crystallization behavior and characteristics of mullites formed from alumina-silica gels prepared by the geopolymer technique in acidic conditions, J. Eur. Ceram. Soc. 21 (2001) 2515–2519.
[24] Z. Liang, Y. Wang, Y. Zhou, H. Liu, Z. Wu, Variables affecting melanoidins removal from molasses wastewater by coagulation/flocculation, Sep. Purif. Technol. 68 (2009) 382–389.
[25] H. Lloyd, A.T. Cooper, M. Fan, R.C. Brown, J. Sawyer, J. van Leeuwen, Y. Shi, N. Li, W. Zhang, Pilot plant evaluation of PFS from coal-fired power plant waste, Chem. Eng. Process. 46 (2007) 257–261.
[26] H.X. Tang, W. Stumm, The coagulating behaviors of Fe(III) polymeric species-I. Preformed polymers by base addition, Water Res. 21 (1987) 115–121.
[27] B. Benyahia, M.A. Latifi, C. Fonteix, F. Pla, S. Nacef, Emulsion copolymerization of styrene and butyl acrylate in the presence of a chain transfer agent, Chem. Eng. Sci. 65 (2010) 850–869.
[28] X. Mei, R. Liu, F. Shen, H. Wu, Optimization of fermentation conditions for the production of ethanol from stalk juice of sweet sorghum by immobilized yeast using response surface methodology, Energy Fuels 23 (2009) 487–491.
[29] M.A. Alim, J.H. Lee, C.C. Akoh, M.S. Choi, M.S. Jeon, J.A. Shin, K.T. Lee, Enzymatic transesterification of fractionated rice bran oil with conjugated linoleic acid: Optimization by response surface methodology, LWT—Food Sci. Technol. 41 (2008) 764–770.
[30] M.S. Secula, G.D. Suditu, I. Poulios, C. Cojocaru, I. Cretescu, Response surface optimization of the photocatalytic decolorization of a simulated dyestuff effluent, Chem. Eng. J. 141 (2008) 18–26.
[31] H. Ceylan, S. Kubilay, N. Aktas, N. Sahiner, An approach for prediction of optimum reaction conditions for laccase-catalyzed bio-transformation of 1-naphthol by response surface methodology (RSM), Bioresour. Technol. 99 (2008) 2025–2031.
[32] B.K. Körbahti, Response surface optimization of electrochemical treatment of textile dye wastewater, J. Hazard. Mater. 145 (2007) 277–286.
[33] S. Ghafari, H.A. Aziz, M.H. Isa, A.A. Zinatizadeh, Application of response surface methodology (RSM) to optimize coagulation–flocculation treatment of leachate using poly-aluminum chloride (PAC) and alum, J. Hazard. Mater. 163 (2009) 650–656.
[34] I. Arslan-Alaton, G. Tureli, T. Olmez-Hanci, Treatment of azo dye production wastewaters using photo-Fenton-like advanced oxidation processes: Optimization by response surface methodology, J. Photochem. Photobiol., A 202 (2009) 142–153.
[35] A. Majumder, A. Goyal, Enhanced production of exocellular glucansucrase from *Leuconostoc dextranicum* NRRL B-1146 using response surface method, Bioresour. Technol. 99 (2008) 3685–3691.

[36] L.V.A. Reddy, Y.J. Wee, J.S. Yun, H.W. Ryu, Optimization of alkaline protease production by batch culture of *Bacillus* sp. RKY3 through Plackett-Burman and response surface methodological approaches, Bioresour. Technol. 99 (2008) 2242–2249.
[37] Y. Li, H. Jiang, Y. Xu, X. Zhang, Optimization of nutrient components for enhanced phenazine-1-carboxylic acid production by gacA-inactivated *Pseudomonas* sp. M18G using response surface method, Appl. Microbiol. Biotechnol. 77 (2008) 1207–1217.
[38] C. Barrera-Díaz, I. Linares-Hernández, G. Roa-Morales, B. Bilyeu, P. Balderas-Hernández, Removal of biorefractory compounds in industrial wastewater by chemical and electrochemical pretreatments, Ind. Eng. Chem. Res. 48 (2009) 1253–1258.